Soft Matter

Accepted Manuscript

This article can be cited before page numbers have been issued, to do this please use: A. A. Pitenis, J. M. Urueña, K. D. Schulze, R. M. Nixon, A. C. Dunn, B. A. Krick, G. Sawyer and T. E. Angelini, *Soft Matter*, 2014, DOI: 10.1039/C4SM01728E.

ROYAL SOCIETY OF CHEMISTRY

www.rsc.org/softmatter

View Article Online
DOI: 10.1039/C4SM01728E

Soft Matter

RSCPublishing

ARTICLE

Polymer Fluctuation Lubrication in Hydrogel Gemini Interfaces

Cite this: DOI: 10.1039/x0xx00000x

A. A. Pitenis,[a] J. M. Urueña,[a] K. D. Schulze,[a] R. M. Nixon,[a] A. C. Dunn,[b] B. A. Krick,[c] W. G. Sawyer[ad] and T. E. Angelini[aef]

Received 00th January 2012,
Accepted 00th January 2012

DOI: 10.1039/x0xx00000x

www.rsc.org/

Interfacial sliding speed and contact pressure between the sub-units of particulate soft matter assemblies can vary dramatically across systems and with dynamic conditions. By extension, frictional interactions between particles may play a key role in their assembly, global configuration, collective motion, and bulk material properties. For example, in tightly packed assemblies of microgels – colloidal microspheres made of hydrogel – particle stiffness controls the fragility of the glassy state formed by the particles. The interplay between particle stiffness and shear stress is likely mediated by particle-particle normal forces, highlighting the potential role of hydrogel-hydrogel friction. Here we study friction at a twinned "Gemini" interface between hydrogels. We construct a lubrication curve that spans four orders of magnitude in sliding speed, and find qualitatively different behaviour from traditional lubrication of engineering material surfaces; fundamentally different types of lubrication occur at the hydrogel Gemini interface. We also explore the role played by polymer solubility and hydrogel-hydrogel adhesion in hydrogel friction. We find that polymer network elasticity, mesh size, and single-chain relaxation times can describe friction at the gel-gel interface, including a transition between lubrication regimes with varying sliding speed.

Introduction

The rheology of dense, particulate, soft matter systems like emulsion droplets, polymer coated hard-sphere colloids, and microgels, forms a rich landscape of strain-dependent and frequency-dependent transitions in material properties.[1, 2] In these soft matter systems, shear forces and normal forces at particle-particle interfaces drive the single-particle rearrangements and the collective motion that often underlie this complex rheology. Locally, at the interface between particles, the ratio of the shear force to the normal force defines a friction coefficient, which also may exhibit strong frequency-dependent transitions. Transitions in friction coefficient have been explored broadly in areas focusing on the lubrication of rigid, impermeable surfaces, like metals, plastics, and ceramics. With engineering materials like these, the interfacial contact between two surfaces moving at a low relative speed is determined by surface roughness; when two opposing surfaces are loaded against one another, the high points of the roughness make contact. The contact stresses at these discrete and minute points of contact are often immense; local stresses are generally assumed to be in the plastic regime and on the order of the material hardness.[3] When there is no fluid present the contact is referred to as "dry." Under these conditions the friction coefficients are typically high (μ>0.2) and the surfaces generally experience significant wear.[4, 5] However, with the addition of fluid and motion, there is a possibility of hydrodynamic lubrication, which, as the name implies, involves the lubrication of the surfaces through the use of fluids in shear. The success or failure of hydrodynamic lubrication critically depends on whether or not the fluid flow can generate enough pressure to completely separate the surfaces from contact (**1a**).

Successful hydrodynamic lubrication is determined by a favourable balance between the film thickening parameters (viscosity, inlet geometry, and sliding speed) and the load or contact pressure, often described by a dimensionless parameter called the Sommerfeld number.[6] Friction between two surfaces is a dynamic process; when a fluid is present, friction coefficients can vary by several orders of magnitude depending on the Sommerfeld number.[7] For engineering materials, the traditional way to illustrate the wide range of friction coefficients is the Stribeck Curve – a plot of friction coefficient versus the Sommerfeld number or versus one of its controlling parameters. There are clear transitions in frictional behaviour, which are well studied and descriptively named based on the operating mechanisms of friction: dry – no fluid is present; boundary lubrication – adsorbed fluid films form on the surfaces reducing friction; mixed lubrication – a transition

View Article Online
DOI: 10.1039/C4SM01728E Journal Name

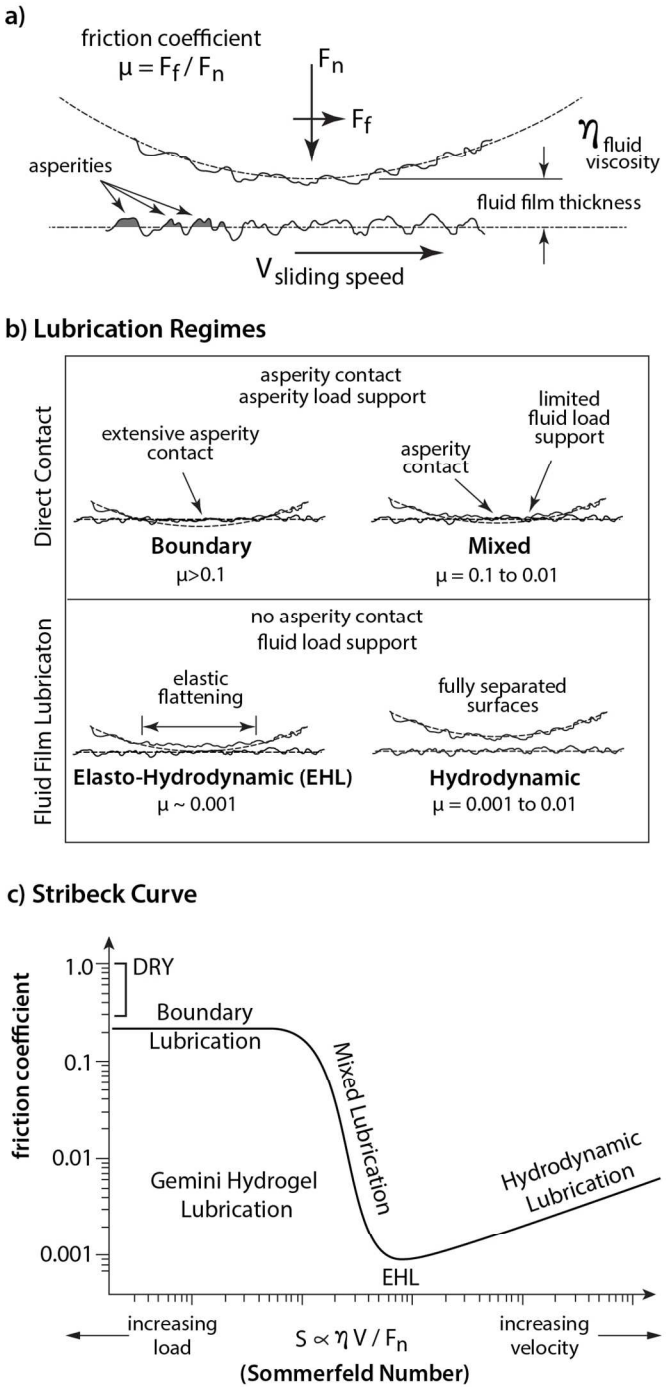

Fig. 1 (a) Schematic of a lubricated sliding interface with pertinent variables shown. (b) Classical lubrication regimes between two sliding surfaces. (c) Classical Stribeck curve with the Gemini hydrogel lubrication regime identified.

between boundary lubrication and fluid film lubrication; elastohydrodynamic lubrication (EHL) – the thinnest fluid film lubrication in which the fluid pressures cause elastic deformations; and hydrodynamic lubrication – a condition of full fluid film lubrication (**1b**). Fluid lubrication theory is only valid when the fluid films are thick enough to completely separate the surfaces; typically, many times thicker than the surface roughness.[8-11] If the same interfacial interactions occur in soft particulate systems, this rich behaviour in the lubrication of rigid, impermeable materials may elucidate the frictional contributions to soft matter rheology. However, the soft matter equivalent of the Stribeck lubrication curve has not yet been explored (**1c**).

Here we investigate transitions in friction at hydrogel-hydrogel interfaces by varying sliding speed to potentially traverse multiple lubrication regimes, and by varying polymer solvation to span a broad range of interfacial interaction strengths. For strongly solvated polymer networks, we find that the hydrogel lubrication behaviour differs qualitatively from the traditional Stribeck curve. Our experiments span four orders of magnitude in sliding speed, over which hydrogel-hydrogel friction coefficients vary only by a factor of four. By contrast, the friction coefficient of traditional engineering interfaces passes through multiple phases of lubrication, spanning at least three orders of magnitude of friction coefficient over the same range of sliding speed. We find that hydrogel friction coefficients are the lowest at slow sliding speeds, exhibiting no equivalent of dry friction even between totally stationary interfaces; static friction between hydrogels is less than or equal to kinetic friction. At high sliding speeds, the friction coefficient exhibits a transition and rises. In contrast to the classical transition into hydrodynamic lubrication, we find that the transition in hydrogels arises from the relaxation time of polymer chain deformation. In collapsed, destabilized hydrogels, friction forces exceed the strength of the polymer networks; adhesive forces at the interfacial contact break hemispherical hydrogel probes from their supports on our instrument. These results suggest a relationship between friction and the rheology of packed microgel phases; at low frequencies friction can be treated as a constant, at high frequencies the friction scales with the interfacial shear rate, and at all frequencies friction is strongly dependent on polymer solvation.

Results

To explore a large breadth of potential frictional mechanisms at the hydrogel-hydrogel interface, we construct an instrument capable of measuring friction over a wide range of interfacial sliding speeds, and we employ a hydrogel with a tunable interfacial energy. Two poly(N-isopropylacrylamide) (pNIPAM) hydrogels of identical composition are synthesized. One hydrogel is cast as a 4.5 mm thick disk and fixed to a rotating stage; the opposing gel is moulded as a half-spherocylinder with a 4 mm diameter shaft and a hemispherical tip with a 2 mm radius of curvature. The gel composition is 7.5% NIPAM, cross-linked with 0.3% bisacrylamide. pNIPAM is a thermosensitive gel that shrinks with increasing temperature; the polymer chains become unstable at temperatures above their lower critical solvation temperature (LCST), approximately 32°C.[12, 13] To measure friction, the hemispherical hydrogel probe is lowered onto the hydrogel countersurface, applying a normal force, F_n, of 2 mN.

Soft Matter

View Article Online
DOI: 10.1039/C4SM01728E ARTICLE

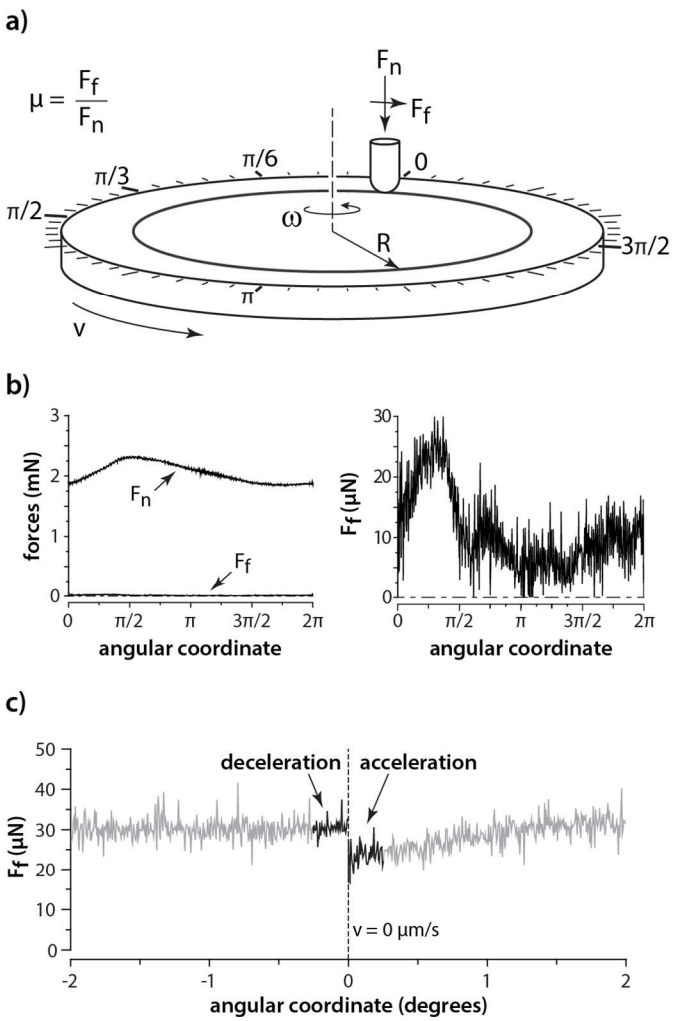

Fig. 2 (a) Schematic of a stationary hydrogel probe sliding against a rotating hydrogel disk in a Gemini hydrogel configuration. (b) Left: Normal (F_n) and friction (F_f) forces measured by capacitance sensors in the normal and the tangential direction, respectively, for a representative cycle (1 rotation). Right: The friction (tangential) force is two orders of magnitude lower than the corresponding normal force. (c) Friction forces for a representative cycle showing no static friction.

The hydrogel sheet is rotated beneath the probe and both the normal force and the tangential friction force, F_f, are measured over time. Sliding speeds are varied either by changing the rotation rate of the support stage or by positioning the probe hydrogel at different radial distances from the centre of rotation. (**2a**)

For highly solvated pNIPAM gels at 26°C sliding at slow speeds, $v < 5$ mm s^{-1}, F_n varies by about +/-0.25 mN. This range in F_n arises from vertical variations in the surface of the hydrogel sheet relative to the rotating support stage. From the vertical cantilever stiffness of 155 μN/μm we determine that this range of normal forces corresponds to a vertical variation of +/-1.6μm over the sliding circumference of 10.7 mm, or an angular misalignment of only 0.15 mrad.

Friction coefficient, μ, is determined by the ratio F_f / F_n. At each sliding speed, both the normal and frictional forces are measured at a rate of 200 Hz for 100 s, yielding 2×10^4 measurements of μ, which are averaged. At slow sliding speeds, F_f is about two orders of magnitude smaller than F_n, yielding friction coefficients of order μ ~0.01 with a standard deviation of 0.003. We observe that the friction force at the start of rotation is always slightly lower than during sliding, demonstrating that static friction is less than kinetic friction at Gemini hydrogel contacts; classical friction exhibits the exact opposite behaviour (**2c**).

Friction transitions with sliding speed

Friction at the interfaces of traditional, stiff, impermeable, engineering materials varies non-monotonically, and often dramatically, with sliding speed. The friction coefficient for a single pair of materials in frictional contact can vary by more than two orders of magnitude with less than an 5-fold change in sliding speed when crossing though the mixed regime of lubrication. By contrast, the friction coefficient can exhibit negligible variation with more than 10-fold change in sliding speed in the boundary lubrication regime, where sliding speeds are low. At the highest sliding speeds, hydrodynamic lubrication is weakly speed-dependent and can be controlled by the viscosity of the lubricating fluid. To explore the possibility that friction at Gemini hydrogel interfaces pass through multiple lubrication transitions, we measure the friction coefficient between two pNIPAM gels at many sliding speeds, spanning a range from 0.03 through 100 mm s^{-1} as shown in Fig. 3.

In stark contrast to the traditional Stribeck curve that shows high friction behaviour at low sliding speeds and low friction behaviour at high sliding speeds, the Gemini-hydrogel lubrication curve exhibits the lowest friction coefficient at slow sliding speeds, with μ ~0.01. This extremely low friction coefficient does not show any significant variation with increasing sliding speed up to about 5 mm s^{-1}. Insight into this rate independence is gained by considering the mechanics of indentation in the limit of no sliding. Since the hydrogels are permeable, flow may be driven out of the indented volume. With an estimated mesh size of 20 nm and applied pressure in the kPa range, the timescale for driving the indented volume of fluid through the network is ~100 s.[14, 15] The hemispherical hydrogel probe is in contact with the counter-surface for much longer times than 100 s, though the countersurface experiences contact only transiently. With the observed interfacial contact diameter of ~1 mm, we predict an upper limit for the speed at which a region of contact remains under pressure for sufficient time to drive fluid flow to be 0.01 mm s^{-1}. Thus, at sliding speeds above 0.01 mm s^{-1} the dominating deformation mode in the lower hydrogel slab is most likely shear strain, which doesn't involve large scale fluid transport relative to the polymer mesh.

We consider the potential contribution of elastic deformations to the measured friction force by estimating the shear stress under the contact. For a hemispherical indentation, the strain is $0.2aR^{-1} = 0.05$, where $a = 0.5$ mm is the contact radius and $R = 2$ mm is the radius of curvature of the hydrogel probe. The contact radius is directly measured by microscopy. We measure the elastic shear modulus,

ARTICLE View Article Online
DOI: 10.1039/C4SM01728E Journal Name

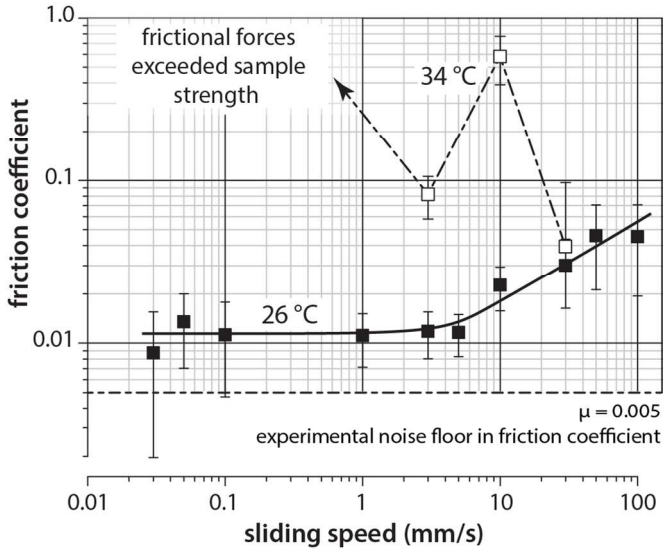

Fig. 3 Friction coefficient plotted versus sliding speed at two temperatures, 26°C and 34°C. Measurements performed at 26°C, represented by black squares, exhibit a low friction coefficient of 0.01 for sliding speeds ranging from 0.03 – 5 mm s^{-1}. At faster sliding speeds the friction coefficient increases to ~0.045. In measurements performed at 34°C, represented by open squares, the friction coefficient is high and erratic; at speeds below 1 mm s^{-1} the frictional forces exceed the strength of the pNIPAM probe.

$G'(\omega)$, in oscillatory rheology over a wide frequency range spanning the corresponding timescales of substrate-probe interaction. In this frequency range of 0.01-10 Hz, measured at strain amplitudes of 1, 5, and 10%, we find that G' = 1 kPa and is frequency independent. In the linear elastic regime, material properties like shear modulus are independent of applied stresses, so we do not expect that G' depends significantly on normal force. The shear stress during sliding is the product of G' and the strain, and the elastic shear force during sliding is the product of the stress and the contact area. By dividing the shear force by the normal force, F_n = 2 mN, we estimate an effective friction coefficient of 0.02. This order-of-magnitude estimate is close to the measured friction coefficient of 0.01, suggesting that the frequency-independent rheology of hydrogels may contribute to the speed-independent friction coefficient at Gemini-hydrogel interfaces. The detailed relationship between slip forces and shear stress at the interface is necessary to understand the underlying origins of the measured friction forces and will be explored in future work. Since dilute gels of flexible polymers derive their material properties from thermal fluctuations, we call this class of friction *thermal fluctuation lubrication.*

The Gemini hydrogel lubrication curve differs qualitatively from the Stribeck curve in another way: at speeds above 5 mm s^{-1}, the friction coefficient rises weakly with sliding speed, scaling like $\mu \sim v^{0.5}$. This scaling can be predicted by a hydrodynamic lubrication theory for an interface with the geometry of the hydrogels used here, but the predicted friction coefficient is over an order of magnitude smaller than our measurements due to the extremely low viscosity of water. Alternatively, this speed dependence could be an artefact of drag forces; the frictional probe is submerged in a deep bath of water that rotates with the lower countersurface. To explore whether these drag forces can deflect the frictional probe, we repeat the experiments with baths of varying depth, finding no sensitivity to the volume of fluid in the bath at all; the same results are found when the bath is reduced to a thin fluid film. We also considered the contribution of viscous stresses in the gel by estimating a friction force arising from $G''(\omega)$. However, these predictions fall several orders of magnitude below the measured forces.

Another potential mechanism of the transition in friction is the relaxation of strained polymer chains at the contact. The relaxation time for flexible chains in a gel is $\tau = \xi^3 \eta / k_B T$, where ξ is the mesh size, η is the solvent viscosity, k_B is Boltzmann's constant, and T is the temperature.[16] For the pNIPAM gel studied here, τ = 2 μs. If the spatial frequency of polymer-polymer strain generation across the sliding contact is ξ^{-1}, then the competing timescale acting against polymer relaxations is ξ / v, where v is the sliding speed. Thus, at the observed transition, v = 5 mm s^{-1}, any point of contact moves by one mesh size in 4 μs. The agreement between these timescales suggests that the transition in frictional behaviour is associated with the ability of polymer thermal fluctuations to relax local deformations before new strains are exerted by the countersurface. We therefore call this type of frictional behaviour *polymer relaxation lubrication*.

Friction transitions with temperature

Thermosensitive hydrogels like pNIPAM are growing in popularity for applications that make use of the strong swelling/de-swelling transition that can occur over a narrow range of temperature or pH.[13] For example, slabs of pNIPAM are used as mechanical actuators in biological applications, and condensed pNIPAM microgel particles are used to study the colloidal glass transition with varying temperature.[17-19] The destabilization of NIPAM polymers is likely to generate large changes in interfacial interactions in cases where multiple pNIPAM gels are in contact.[19]

To explore the role of polymer solvation on Gemini hydrogel friction, the same series of experiments described above are performed, but with the hydrogels equilibrated at 34°C, about 2°C above the LCST of pNIPAM. We find that the pNIPAM interface at high temperature is dramatically different from the same interface between swollen gels at low temperatures. At the slowest sliding speeds, friction forces are so high that the hydrogel probe is torn apart, precluding the possibility of measuring a friction coefficient. When measurements are possible at higher sliding speeds, exceeding 1 mm s^{-1}, the coefficient of friction varies erratically, reaching levels comparable to dry friction. These results highlight the role of thermal fluctuations in solvated hydrogel friction. pNIPAM chains at temperatures above the LCST are not solvated and the frictional mechanisms associated with thermal fluctuations, discussed above, are not acting.

To elucidate the origins of this extremely high friction coefficient at temperatures above the LCST, and the associated transition from low to high friction, we perform a series of force-indentation measurements at multiple temperatures, from 26°C to 37°C. pNIPAM probes are loaded and unloaded against pNIPAM sheets, both identical to those used in friction experiments (Fig 4).

Soft Matter
View Article Online
DOI: 10.1039/C4SM01728E
ARTICLE

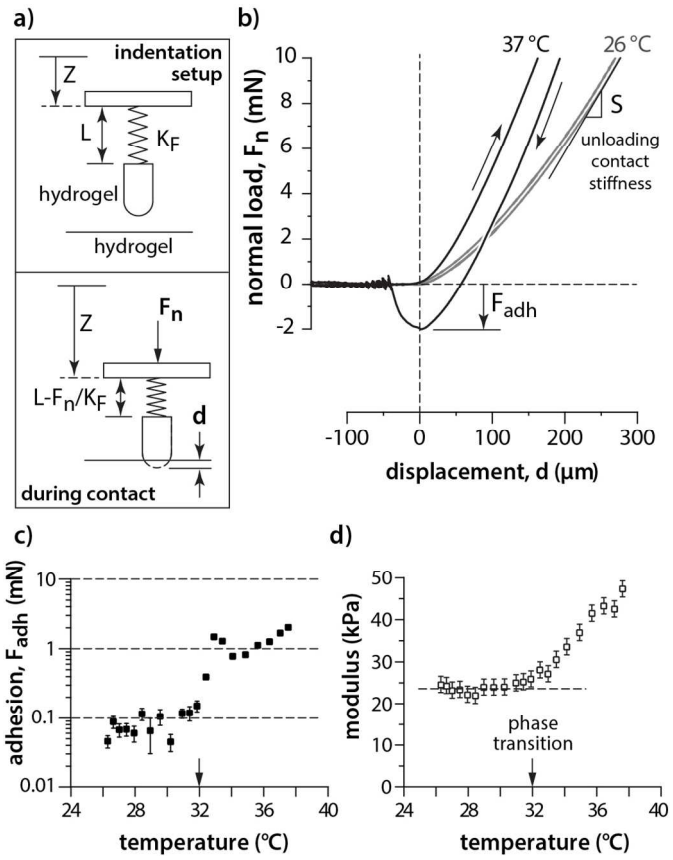

Fig. 4 (a) Representation of hydrogel probe approaching hydrogel sheet prior to indentation, where Z is the reference location from a stationary point on the microtribometer, L is the length of the undeformed cantilever flexure, and K_F is the normal stiffness of the flexure. During contact, the probe indents the sheet by a normal load F_n causing a displacement d, deflecting the flexure by $L-F_n/K_F$. (b) Loading and unloading indentation curves from the lowest and highest tested temperatures exhibit adhesion above the LCST, indicated by the significant negative peak in normal force during retraction. (c) The force of adhesion, F_{adh}, is determined from the lowest value of the normal load during probe retraction. We observe a transition in adhesive force at 32°C (indicated by an arrow) where F_{adh} increases by an order of magnitude. The error bars represent uncertainty in the F_{adh} measurements due to fluctuations in the cantilever deflection. (d) The elastic modulus also exhibits a transition with increasing temperature. Below the transition temperature of 32°C, the modulus is relatively steady around 24 kPa; above 32°C the modulus increases monotonically to 47 kPa.

The probe is loaded against the sheet at a rate of 65 μm s^{-1} until a normal load of 10.7 mN is reached. The probe is retracted at the same rate, resulting in a full loading-unloading duration of about 30 seconds. An adhesion force is measured at every temperature, determined by a negative peak in the unloading force curve. Below the LCST, the adhesion force is approximately constant, fluctuating around 0.05 mN. A sharp jump in adhesion occurs at the LCST, above which the adhesion force is 1-2 mN. These results further suggest that the high friction coefficient at high temperatures is due to hydrogel-hydrogel adhesion.

We determine an effective contact modulus from the indentation curves by employing Johnson-Kendall-Roberts (JKR) theory which incorporates the effect of adhesion in indentation measurements.[20] For each indentation the unloading contact stiffness is calculated by fitting the slope of the unloading curve, S, at a normal load of 9 mN. The total normal force, F_n', is calculated by adding the absolute value of the normal load (9 mN) to the absolute value of the maximum force of adhesion, $F_n' = |F_n|+|F_{adh}|$. The stiffness and the adhesive force are used to calculate the modulus, E, given by $E = ((1-n)^2/2)*(S^3/(3F_n'R))^{0.5}$, where n = 0.3 is the Poisson's ratio of pNIPAM, and R' = 2 mm is the radius of curvature of the probe. This methodology produces systematically repeatable measurements of an effective contact modulus, but is not intended to be directly compared to tests that directly measure shear modulus or Young's modulus. We find that the indentation modulus of pNIPAM gels is constant below the LCST, with an average value of 24 kPa. At the LCST, the modulus rises monotonically, reaching 47 kPa at 37 °C. This trend suggests that the friction coefficient may also be temperature-independent up to the LCST, given the role played by the shear modulus in friction discussed above.

Discussion

Interfacial sliding speed and contact pressure between the sub-units of particulate soft matter assemblies can vary dramatically across systems and contexts. Thus, frictional interactions between particles may play an essential role in their assembly, global configuration, collective motion, and bulk material properties. For example, the extremely low friction between droplets in compressed emulsions allows these systems to remain isostatic under large osmotic pressures, facilitating the measurement of bulk compressibility and the study of packing statistics.[21] In strongly sheared systems of buoyant acrylic particles, hydrodynamic reversibility is broken by the onset of a dynamical phase transition in which particle collisions drive rearrangements and long timescale diffusive particle motion.[22, 23] In this case, the interaction between particles has not been characterized, though it is hypothesized that the surface roughness plays a role, pointing toward friction as a key interaction. Microgels – colloidal microspheres made of hydrogel – have facilitated explorations of the role that particle stiffness can play in colloidal phase transitions.[2, 24, 25] The interplay between particle stiffness and shear stress is likely mediated by particle-particle normal forces and by the Gemini hydrogel friction behaviour described here. In recent work on active-matter systems, osmotic pressure is used to drive the assembly of protein filaments into bundles, in which the filaments slide against one another by the driving forces of molecular motors.[26] The osmotic pressure generates an applied normal force; friction forces may be associated with the adhesive strength and on-off rates of motors, or direct-contact friction forces associated with the surfaces of filament-pairs sliding against one another. In all of these examples at the frontier of soft matter research, the two fundamental forces of

View Article Online
DOI: 10.1039/C4SM01728E
Journal Name

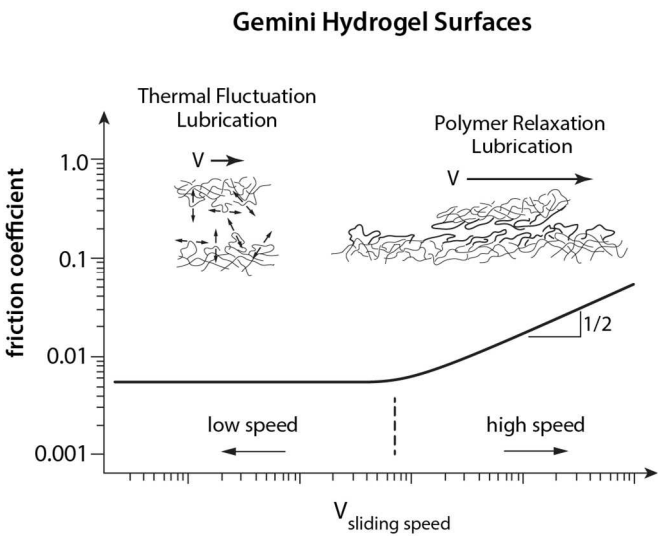

Fig. 5 Gemini hydrogel lubrication model. For low speeds, thermal fluctuation lubrication dominates and the coefficient of friction remains low. For high speeds, polymer relaxation and adhesion are the dominating mechanisms and a corresponding increase of friction coefficient to the ½ power arises.

friction – normal and tangential forces – play a critical role in collective dynamics and macroscopic material properties, highlighting the broad need for tribological investigation in soft matter.

The work described here has direct implications in compressed microgel systems, in which a variety of behaviours are observed at volume fractions higher than close packing. Below the close packing volume fraction, monodisperse microgels crystallize to maximize entropy like hard sphere colloidal crystals, fluctuating within their unit cells.[25, 27] At volume fractions above close packing the microgels compress, make intimate contacts with their neighbours, and deform at their surfaces to fill open space. The fluctuations of compressed microgels and the macroscopic rheological properties of compressed microgel assemblies have been shown to depend on both the bulk modulus and the shear modulus of the microgel particles, highlighting the importance of normal forces, shear forces, and consequently the friction coefficient at particle-particle interfaces.[24, 28]

In systems of polydisperse microgels, the particles do not crystallize, but form colloidal glasses instead.[2] Remarkably, the fragility of these soft colloidal glasses is controlled by the stiffness of the microgel particles; stiffer particles form more fragile glasses, and softer particles form stronger glasses. Many different polymer chemistries have been used to study microgel physics, and pNIPAM is frequently used. Very often the pNIPAM microgels are copolymerized with negatively charged groups to prevent the adhesion that we observe here with pNIPAM above the LCST. Interestingly, in molecular glasses, molecules that form strong bonds with one another tend to form fragile glasses, whereas molecules that can easily break bonds with their neighbours tend for form stronger glasses.[29] Thus, the dramatic changes in friction coefficient and adhesion that occur with temperature-dependent gel collapse, observed here, suggest that fragility in compressed microgel systems may also be controlled by friction. We believe that future explorations of adhesion and friction in soft colloidal glasses may help to further elucidate the fundamental origins of the glass transition.

Gemini hydrogel friction mirrors the lubrication of solvated polymer brush interfaces in some ways, and differs from it in other ways[30-32]. Pioneering studies of polymer brushes attached to mica surfaces and measured in a surface force apparatus (SFA) showed that polymer brushes have extremely low kinetic friction (μ<0.001) at low sliding speeds (v~450 nm s^{-1}), and exhibit no measurable static friction at the onset of sliding.[33] Much like Gemini hydrogel friction described here, this behaviour is attributed to polymer chain fluctuations. By contrast, the lubrication curve of the polymer brush interface, when measured in a macro-tribometer, resembles the classic Stribeck curve at higher sliding speeds, above 1 mm s^{-1}.[34] In both macro-tribometry and SFA measurements, the polymer density is approximately the same as the hydrogels studied here, so the differences between Gemini hydrogel lubrication and polymer brush lubrication may arise from the major role of boundary conditions imposed by the rigid surfaces onto which polymer brushes are grafted. As brush surfaces are pressed against one another, the polymer concentration rises dramatically, effectively stiffening the brush and generating a much stronger force-displacement rise than in bulk hydrogels at the same polymer concentration. Consequently, at normal loads in the range of mN, the contact area between brushes is much lower than between bulk hydrogels, resulting in MPa to GPa pressures between brushes; the bulk hydrogels studied here are effectively semi-infinite half-spaces which allow large-lengthscale shear strain to spread throughout the gel, resulting in kPa pressures between contacting hydrogels.[33]

We have shown that Gemini hydrogel friction has strong, qualitative differences from classical friction at stiff, impermeable, lubricated interfaces (Fig. 5). The connection between Gemini hydrogel friction, polymer network stiffness, and chain relaxation time, suggests that mesh size is a key control parameter in the Gemini hydrogel lubrication curve. The twinned, "Gemini" nature of the interface is essential to the shape of this lubrication curve; moving a curved impermeable surface against a flat hydrogel, or a curved hydrogel against a flat impermeable surface produces friction with speed- and time-dependence dramatically different from Gemini hydrogel friction.[15]

Much of the current thought on friction between soft, permeable materials was developed through many decades of research on cartilage.[35-39] Unfortunately, cartilage is an incredibly complicated system, involving stratified layers of fibres with varying structure, mesh size, charge density, and material properties. This high degree of complexity makes the problem of uncovering the fundamentals of lubrication between soft, permeable surfaces practically intractable. Consequently, a great number of models attempting to describe lubrication at soft, permeable interfaces have been developed based on measurements of cartilage friction, creating continual

Soft Matter
View Article Online
DOI: 10.1039/C4SM01728E
ARTICLE

controversy that remains unsettled. The exquisite level of control over physical and chemical properties in synthetic hydrogel systems facilitates the exploration of the models of friction proposed in cartilage research. The work described here revealing a class of lubrication qualitatively different from classical lubrication and from hypothesized modes of friction in cartilage highlights the need for broad exploration of friction in highly controlled, synthetic, Gemini hydrogel interfaces.

Materials and Methods

Experimental apparatus

The apparatus used for these experiments was a high-speed, pin-on-disk, unidirectional microtribometer. The hydrogel probe (2 mm radius of curvature) was adhered directly to a single flexure cantilever assembly, which had a normal stiffness of 155 μN/μm and a lateral stiffness of 74 μN/μm. The probe was loaded to 2 mN by a vertical coarse positioning micrometer against a hydrogel countersample (~4.5 mm in thickness), which was adhered directly to the rotary stage. The high-speed piezoelectric rotary stage (Physik Instrumente M-660.55, 4 μrad resolution) was used to rotate the hydrogel countersample, and was capable of unidirectional angular velocities from 1 to 720 degrees per second. Two 3 mm capacitive displacement sensors measured the displacement of the flexure due to normal and lateral forces during contact and sliding. One was mounted axially with respect to the hydrogel probe to measure normal forces and the other was parallel with respect to the sliding direction of the hydrogel probe to measure friction forces. Each capacitance sensor had a 20 V range and a sensitivity range of 5 μm/V.

Hydrogel preparation

Hydrogel samples were made by polymerizing the following components, reported as mass-per-mass of solvent: NIPAM monomer (7.5%), ammonium persulfate initiator (0.6%), N,N'-Methylenebisacrylamide cross-linker (0.3%), and tetramethylethylenediamine catalyst (0.06%) in ultrapure water and in an oxygen-starved environment at room temperature for 2 hours. The pNIPAM probe and sheet were equilibrated in ultrapure water for 24 hours, during which negligible swelling or shrinking was observed.

To create the Gemini interface, a diamond-turned polyolefin mould was used to cast the probes. Polystyrene petri dishes were used to cast the countersamples. Hemispherical probes of 2 mm radius of curvature and disk-shaped countersamples of ~4.5 mm thickness and 30 mm radius were moulded. A 10 mm stroke radius was selected for sliding speeds of 1 – 100 mm s^{-1} and a 1.7 mm stroke radius was chosen for 0.03 – 0.1 mm s^{-1} sliding speeds due to the velocity limits of the rotary stage.

Acknowledgements

This work was funded by Alcon Laboratories.

Notes and References

[a]Department of Mechanical and Aerospace Engineering
University of Florida, Gainesville, Florida 32611
[b] Department of Mechanical Science and Engineering
University of Illinois at Urbana-Champaign, Urbana, Illinois 61801
[c] Department of Mechanical Engineering and Mechanics
Lehigh University, Bethlehem, Pennsylvania 18015
[d] Department of Materials Science and Engineering
University of Florida, Gainesville, Florida 32611
[e] J. Crayton Pruitt Family Department of Biomedical Engineering
University of Florida, Gainesville, Florida 32611
[f] Institute for Cell Engineering and Regenerative Medicine, Gainesville, Florida 32611

1. R. G. Larson, *The Structure and Rheology of Complex Fluids*, Oxford University Press New York, 1999.
2. J. Mattsson, H. M. Wyss, A. Fernández-Nieves, K. Miyazaki, Z. Hu, D. R. Reichman and D. A. Weitz, *Nature*, 2009, **462**, 83-86.
3. J. Archard, *Journal of Applied Physics*, 1953, **24**, 981-988.
4. M. Antler, *Wear*, 1964, **7**, 181-203.
5. J. Archard and W. Hirst, *Proceedings of the Royal Society of London. Series A. Mathematical and Physical Sciences*, 1956, **236**, 397-410.
6. M. C. Shaw and T. J. Nussdorfer, *National Advisory Committee for Aeronautics (NACA) Report No. 866*, 1947.
7. R. Stribeck and M. Schröter, *Die wesentlichen Eigenschaften der Gleit-und Rollenlager: Untersuchung einer Tandem-Verbundmaschine von 1000 PS*, Springer, 1903.
8. F. P. Bowden and D. Tabor, *Friction: An Introduction to Tribology*, RE Krieger Publishing Company, 1982.
9. D. Dowson, *History of Tribology*, Longman London, 1979.
10. B. J. Hamrock, S. R. Schmid and B. O. Jacobson, *Fundamentals of Fluid Film Lubrication*, CRC press, 2004.
11. J. A. Tichy, *Tribology Transactions*, 1995, **38**, 108-118.
12. M. Heskins and J. E. Guillet, *Journal of Macromolecular Science: Part A - Chemistry*, 1968, **2**, 1441-1455.
13. H. Schild, *Progress in Polymer Science*, 1992, **17**, 163-249.
14. T.-P. Hsu and C. Cohen, *Polymer*, 1984, **25**, 1419-1423.
15. A. C. Dunn, W. G. Sawyer and T. E. Angelini, *Tribology Letters*, 2014, **54**, 59-66.
16. P.-G. De Gennes, *Scaling Concepts in Polymer Physics*, Cornell University Press, 1979.
17. M. E. Harmon, M. Tang and C. W. Frank, *Polymer*, 2003, **44**, 4547-4556.
18. J. F. Mano, *Advanced Engineering Materials*, 2008, **10**, 515-527.
19. H. Senff and W. Richtering, *The Journal of Chemical Physics*, 1999, **111**, 1705-1711.
20. K. Johnson, K. Kendall and A. Roberts, *Proceedings of the royal society of London. A. mathematical and physical sciences*, 1971, **324**, 301-313.
21. I. Jorjadze, L.-L. Pontani and J. Brujic, *Physical Review Letters*, 2013, **110**, 048302.

View Article Online
DOI: 10.1039/C4SM01728E
Journal Name

22. L. Corte, P. Chaikin, J. Gollub and D. Pine, *Nature Physics*, 2008, **4**, 420-424.
23. L. Corté, S. J. Gerbode, W. Man and D. Pine, *Physical review letters*, 2009, **103**, 248301.
24. B. Sierra-Martín, Y. Laporte, A. South, L. Lyon and A. Fernández-Nieves, *Physical Review E*, 2011, **84**, 011406.
25. L. A. Lyon and A. Fernandez-Nieves, *Annual Review of Physical Chemistry*, 2012, **63**, 25-43.
26. T. Sanchez, D. T. Chen, S. J. DeCamp, M. Heymann and Z. Dogic, *Nature*, 2012, **491**, 431-434.
27. B. Sierra-Martín and A. Fernández-Nieves, *Soft Matter*, 2012, **8**, 4141-4150.
28. J. J. Liétor-Santos, B. Sierra-Martín and A. Fernández-Nieves, *Physical Review E*, 2011, **84**, 060402.
29. C. A. Angell, *Science*, 1995, **267**, 1924-1935.
30. S. Lee, M. Müller, M. Ratoi-Salagean, J. Vörös, S. Pasche, S. M. De Paul, H. A. Spikes, M. Textor and N. D. Spencer, *Tribology Letters*, 2003, **15**, 231-239.
31. S. Lee, M. Müller, R. Heeb, S. Zürcher, S. Tosatti, M. Heinrich, F. Amstad, S. Pechmann and N. Spencer, *Tribology Letters*, 2006, **24**, 217-223.
32. C. Perrino, S. Lee and N. D. Spencer, *Tribology Letters*, 2009, **33**, 83-96.
33. J. Klein, E. Kumacheva, D. Mahalu, D. Perahia and L. J. Fetters, *Nature*, 1994, **370**, 634-636.
34. P. C. Nalam, J. N. Clasohm, A. Mashaghi and N. D. Spencer, *Tribology Letters*, 2010, **37**, 541-552.
35. G. Ateshian, H. Wang and W. Lai, *Journal of Tribology*, 1998, **120**, 241-248.
36. C. W. McCutchen, *Wear*, 1962, **5**, 1-17.
37. V. Mow, S. Kuei, W. Lai and C. Armstrong, *Journal of biomechanical engineering*, 1980, **102**, 73-84.
38. M. Caligaris and G. A. Ateshian, *Osteoarthritis and Cartilage*, 2008, **16**, 1220-1227.
39. H. Forster and J. Fisher, *Proceedings of the Institution of Mechanical Engineers, Part H: Journal of Engineering in Medicine*, 1996, **210**, 109-119.